

## Lattice defect and oxygen self-diffusion in MgO-stabilized ZrO<sub>2</sub>

KEN ANDO, Y. OISHI, H. KOIZUMI, Y. SAKKA

*Department of Nuclear Engineering, Kyushu University, Fukuoka 812, Japan*

Electrical conductivity of various stabilized ZrO<sub>2</sub> has been determined by many investigators. In contrast, direct determination of oxygen self-diffusion by the tractor technique has been performed for only CaO-stabilized ZrO<sub>2</sub> by Kingery *et al.* [1] at 680 to 890°C and by Simpson and Carter [2] at 800 to 1100°C. Since these temperature ranges are within two-phase regions, according to the recent CaO–ZrO<sub>2</sub> phase diagram [3], those oxygen self-diffusion coefficients are interpreted to have been determined at a metastable state.

The present work was undertaken to determine the oxygen self-diffusion in MgO–ZrO<sub>2</sub> solid solution to clarify the diffusion mechanism by comparing the results with those of CaO-stabilized ZrO<sub>2</sub>. The determination was extended from two-phase regions to the single-cubic phase region toward high temperatures. Since the phase transition rate on cooling is known to be higher in the MgO–ZrO<sub>2</sub> system than in the CaO–ZrO<sub>2</sub> system [4], the effect of phase transition from the cubic form to the two-phase state on the oxygen self-diffusion is expected to be elucidated better for the MgO–ZrO<sub>2</sub> solid solution.

Two types of lattice defect, oxygen vacancy and cation interstitial, were reported for a cubic CaO–ZrO<sub>2</sub> solid solution [5]. To confirm the lattice defect type for the employed MgO–ZrO<sub>2</sub> solid solutions, a density measurement was conducted.

Samples were prepared from mixed powders of and ZrO<sub>2</sub> (99.6% pure). Mixed powder for a designed composition was pressed into a disc shape and sintered at 2200°C for 3 h in an argon atmosphere. The sintered pellet was annealed in air at 1800°C for 4 h and subsequently quenched by dropping into an ice and water bath. The quenched sample was crushed and ground using an agate mortar and subjected to the pycnometric density measurement and X-ray diffraction.

Samples were prepared from mixed powders of MgO and ZrO<sub>2</sub> for the designed compositions. The mixed powders were isostatically pressed under a pressure of 7 ton cm<sup>-2</sup>, subsequently ground into a spherical shape and sintered at 1750°C for 3 h in air. Densities of sintered samples for four compositions ranged from 93 to 95% of the theoretical densities calculated for the lattice defect type which was determined later. The samples were heat-treated again at 1580°C for 2 h to stabilize the microstructure of the fluorite-cubic phase. After quenching to room temperature, samples were ground and finished into spheres of 6 to 7 mm diameter using SiC paper and subjected to the oxygen self-diffusion coefficient determination. Three compositions (12.0, 14.0, and 16.0 mol % MgO) and temperatures employed for the determination are plotted on Grain's phase diagram [6] as shown in Fig. 1.

The oxygen self-diffusion coefficient was determined by the isotope exchange technique using <sup>18</sup>O as the tracer. Before the diffusion experiment the sphere sample was pre-annealed in a natural oxygen atmosphere for 20 min at the same temperature under the same O<sub>2</sub> pressure (180 torr) as in the diffusion anneal. Diffusion annealing was conducted using a high-frequency induction furnace with a Pt–Rh susceptor. The <sup>18</sup>O concentrations decreasing in the gas phase were determined at scheduled intervals during the diffusion anneal by means of a mass-spectrometer. The diffusion coefficient was calculated from the <sup>18</sup>O diffusion amount using a diffusion equation for the boundary condition where diffusion from a well-stirred fluid of a fixed volume into a sphere was controlled by the surface exchange rate [7].

In Fig. 2 are shown the densities determined for samples of the four compositions quenched from 1800°C in air into an ice-water bath, where the results are compared with theoretical densities (solid lines) calculated with the assumption of the

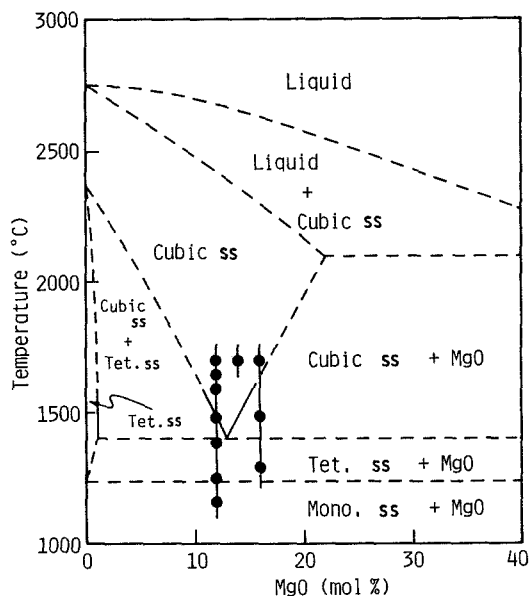


Figure 1 Compositions and temperatures for determination of oxygen self-diffusion coefficient plotted on Grain's MgO-ZrO<sub>2</sub> phase diagram [6].

anion-vacancy type and cation-interstitial type solid solutions, respectively. The results indicate that oxygen vacancies are the predominant lattice defect in the present cubic MgO-ZrO<sub>2</sub> solid solutions at 1800°C.

Oxygen self-diffusion coefficients determined for 12MgO·88ZrO<sub>2</sub> are shown by closed circles as a function of temperature in Fig. 3, where phase boundary temperatures read from the phase diagram [6] are indicated by dashed lines. The whole diffusion coefficients can not be properly represented by a single Arrhenius equation, but the four data in the single-cubic phase region can be represented by

$$D = 1.02 \times 10^{-8}$$

$$\times \exp [-62.8(\text{kJ mol}^{-1})/RT] \text{ m}^2 \text{ sec}^{-1} \quad (1)$$

In comparison with the extrapolation of those results (dotted line), as the temperature decreases, oxygen self-diffusion coefficients tend to deviate toward the lower side with increasing apparent activation energy.

Oxygen self-diffusion coefficients determined for 14MgO·86ZrO<sub>2</sub> and 16MgO·84ZrO<sub>2</sub> are similarly shown by squares and triangles, respectively in Fig. 4 where the solid line represents the results for 12MgO·88ZrO<sub>2</sub> in Fig. 3. As compared at 1697°C, the three different samples do not reveal significant composition dependence of the

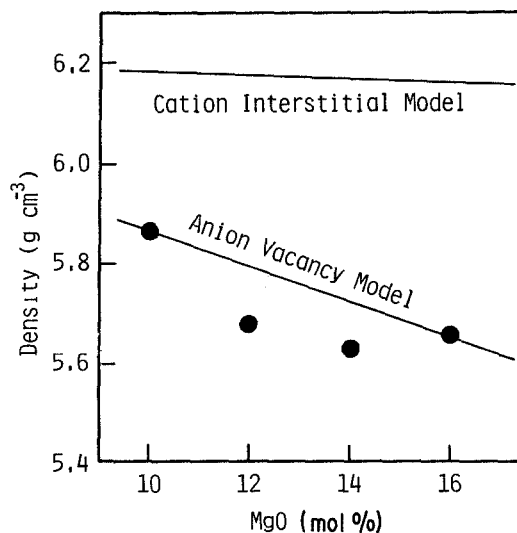
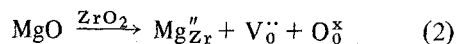


Figure 2 Pycnometric densities in comparison with theoretical densities for two defect types of MgO-ZrO<sub>2</sub> solid solutions.

oxygen self-diffusion coefficient. Although the number of determinations is limited for 16MgO·84ZrO<sub>2</sub>, the temperature dependence of the oxygen diffusion with respect to phase transition is understood to be similar to the 12MgO·88ZrO<sub>2</sub> case.

Regarding the lattice defect type in the fluorite-cubic CaO-ZrO<sub>2</sub> solid solution, according to Diness and Roy [5], and Carter and Roth [8], oxygen vacancies are the predominant defect in the low temperature range, while interstitial cations are predominant in the relatively high temperature range. Since the ionic radius of the magnesium ion is smaller than that of the calcium ion, one may expect the possibility of interstitial cations to occur more in the MgO-ZrO<sub>2</sub> system than in the CaO-ZrO<sub>2</sub> system. However, as shown in Fig. 2, the predominance of the oxygen vacancy type was confirmed at 1800°C for the composition range of 10 to 16 mol % MgO. At temperatures lower than 1800°C, the oxygen vacancy type is expected to remain predominant by analogy with CaO-stabilized ZrO<sub>2</sub> in which occurrence of the interstitial cation types is limited to only relatively high temperatures [5]. Consequently, formation of a lattice defect in MgO-ZrO<sub>2</sub> solid solution is primarily described by Equation 2 in the Kroger-Vink notation.



The diffusion samples were equilibrated at

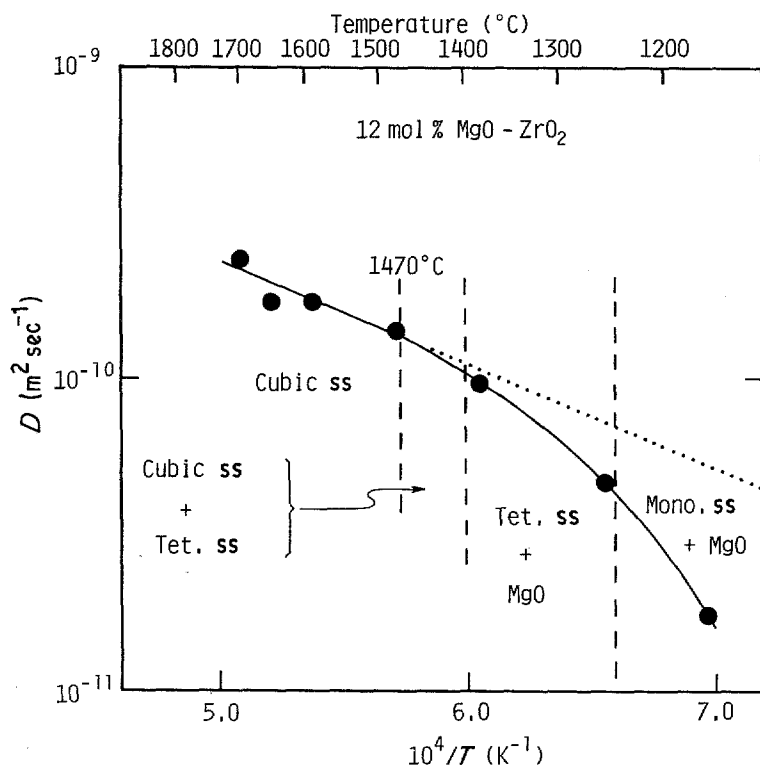


Figure 3 Oxygen self-diffusion coefficients for  $12\text{MgO}\cdot 88\text{ZrO}_2$  as a function of temperature.

$1580^\circ\text{C}$  prior to the diffusion experiments. No appreciable phase transition is expected to proceed from the single-cubic phase state during the pre-annealing and diffusion anneal, since cationic interdiffusions required for those phase transitions are slow [9]. However, deviations of the temperature dependences of oxygen self-diffusion coefficients in low temperature ranges shown in Figs. 3 and 4 appear to be corresponding to phase transitions indicated in the phase diagram.

With respect to the composition  $12\text{MgO}\cdot 88\text{ZrO}_2$ , as seen in Figs. 1 and 3, the fluorite cubic phase is stable at temperatures higher than  $1470^\circ\text{C}$ ; the temperature range  $1470$  to  $1400^\circ\text{C}$  is a two-phase region for fluorite-cubic and tetragonal solid solutions; the temperature range  $1400$  to  $1240^\circ\text{C}$  is a two-phase region for the tetragonal solid solution and MgO; the temperature range lower than that is a two-phase region for the monoclinic solid solution and MgO.

As shown in Fig. 3, the oxygen self-diffusion coefficient exhibits a break in its temperature dependence at  $1400^\circ\text{C}$  where the fluorite-cubic phase with high MgO content disappears and the tetragonal phase with reduced MgO content and the MgO phase are formed. If this transition takes place, it should result in a substantial decrease of

oxygen vacancy concentration and consequently, in low oxygen diffusivity.

In the higher temperature range  $1470$  to  $1400^\circ\text{C}$ , the tetragonal phase occurs in the host cubic phase. However, as seen in Fig. 1, the substantial fraction in the phase composition here is the cubic phase, which is the continuous phase and primarily determines the oxygen diffusivity of the overall system. Thus, even if that phase transition takes place, the normally expected oxygen diffusivity is not necessarily pronounced in this temperature range, which appears to be the case in Fig. 3. The pronounced decrease in oxygen diffusion from the tetragonal phase plus MgO region to the monoclinic phase plus MgO region, shown in Fig. 3, is interpreted to be due to the higher oxygen diffusivity in the tetragonal solid solution than in the monoclinic solid solution which has lower MgO solubility than the tetragonal phase.

As mentioned earlier, the oxygen self-diffusion in the single fluorite-cubic phase region above  $1470^\circ\text{C}$  is described by Equation 1. Its comparison with the  $16\text{MgO}\cdot 84\text{ZrO}_2$  data in Fig. 4 does not seem to indicate a pronounced difference in the magnitude of the activation energy in this single-cubic phase region. The activation energy,  $62.8\text{ kJ mol}^{-1}$ , is interpreted to be the migration energy of

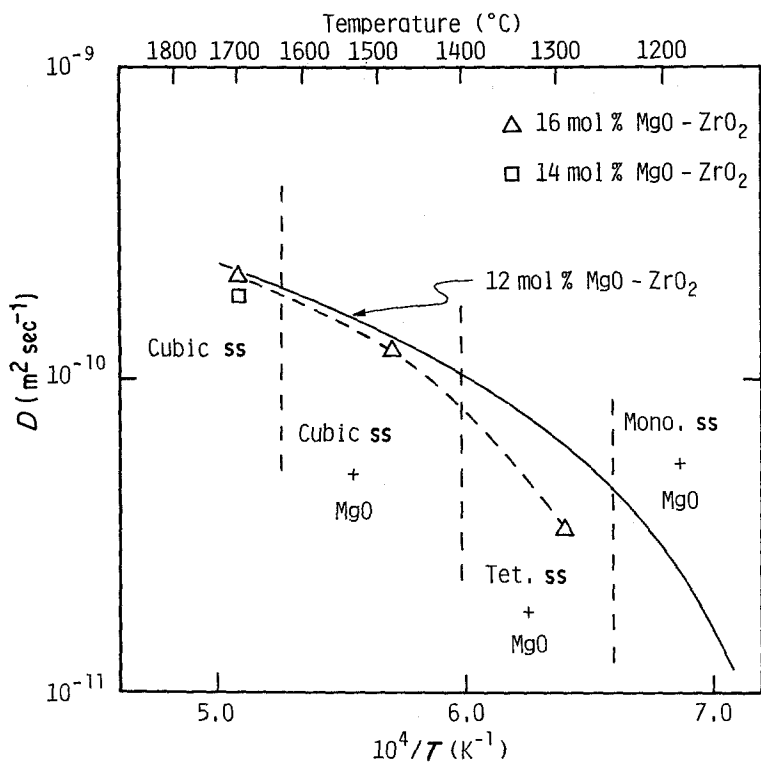


Figure 4 Oxygen self-diffusion coefficients for 16MgO·84ZrO<sub>2</sub> as a function of temperature.

the oxygen ion typical of the fluorite-cubic MgO-ZrO<sub>2</sub> solid solution. (Defect association which might be relevant to the problem is not discussed here.)

The temperature dependence of the diffusion coefficients below 1400°C for 12MgO·88ZrO<sub>2</sub>,

shown in Fig. 3, may be expressed as an activation energy of approximately 150 kJ mol<sup>-1</sup>. As discussed above, however, this activation energy has no physical meaning for a simple self-diffusion but varies depending on the thermal history of the samples.

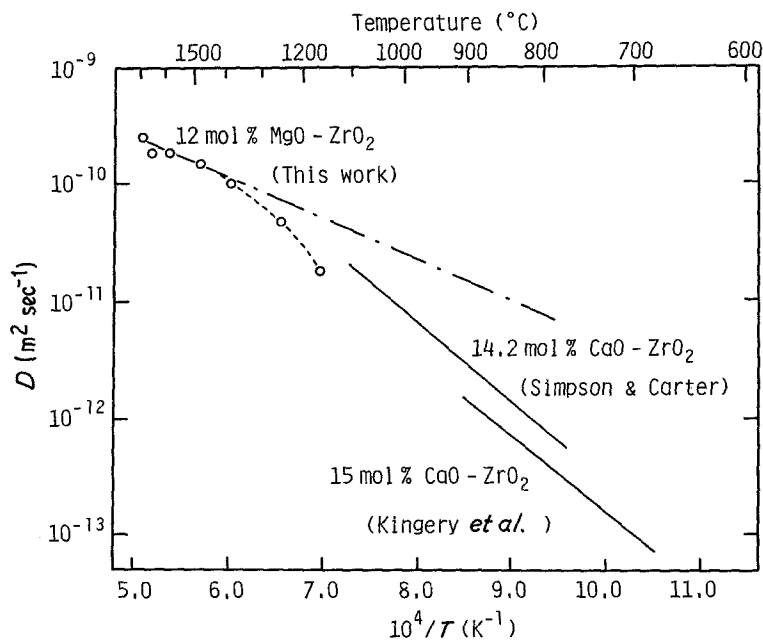


Figure 5 Comparison of oxygen self-diffusion coefficients in systems MgO-ZrO<sub>2</sub> and CaO-ZrO<sub>2</sub>.

With respect to the composition  $16\text{MgO}\cdot 84\text{ZrO}_2$ , the oxygen self-diffusion coefficient exhibits no significant change from the single-cubic phase region to the two-phase region of the cubic and MgO phases, as compared with  $12\text{MgO}\cdot 88\text{ZrO}_2$  in Fig. 4. This can be explained in a similar manner to the cubic plus tetragonal region of  $12\text{MgO}\cdot 88\text{ZrO}_2$ , that is, as seen in the phase diagram, the substantial fraction in the phase composition here is the cubic solid solution, which is the continuous phase and primarily determines the oxygen diffusivity of the overall system; the MgO phase with low diffusivity [10] is an isolated phase in the host cubic solution. The pronounced decrease of the oxygen diffusion coefficient from the cubic solid solution plus MgO region to the tetragonal solid solution plus MgO region was already explained for  $12\text{MgO}\cdot 88\text{ZrO}_2$ , except that this phase transition effect appears to be more pronounced in the solid solution with higher MgO content.

The oxygen self-diffusion coefficients determined for  $12\text{MgO}\cdot 88\text{ZrO}_2$  are compared in Fig. 5 with those for CaO-stabilized  $\text{ZrO}_2$  in the literature. The activation energy for the single-cubic phase region of  $12\text{MgO}\cdot 88\text{ZrO}_2$ ,  $62.8\text{ kJ mol}^{-1}$ , is similar in magnitude to the migration energy of the oxygen vacancy for  $\text{ZrO}_2$ -based crystals,  $66\text{ kJ mol}^{-1}$ , reported in a review by Kilner and Brook [11]. The magnitudes of these activation energies are approximately one half of those determined for the oxygen diffusion in  $15\text{CaO}\cdot 85\text{ZrO}_2$  ( $127\text{ kJ mol}^{-1}$ ) [1] and  $14.2\text{CaO}\cdot 85.8\text{ZrO}_2$

( $131\text{ kJ mol}^{-1}$ ) [2]. The migration energy of the oxygen vacancy in a fluorite-cubic oxide is primarily determined by the host cation and is not sensitive to dopant cations [11]. Those high activation energies determined for CaO-stabilized  $\text{ZrO}_2$  are understood to involve energy other than the migration energy of the single oxygen vacancy.

## References

1. W. D. KINGERY, J. PAPPIS, M. E. DOTY and D. C. HILL, *J. Amer. Ceram. Soc.* **42** (1959) 393.
2. L. A. SIMPSON and R. E. CARTER, *ibid.* **49** (1966) 139.
3. J. R. HELLMANN and V. S. STUBICAN, *ibid.* **66** (1983) 260.
4. R. C. GARVIE, in "High Temperature Oxides" Vol. 5, II, edited by A. M. Alper (Academic Press, New York, 1970) p. 117.
5. A. M. DINESS and R. ROY, *Solid State Commun.* **3** (1965) 123.
6. C. F. GRAIN, *J. Amer. Ceram. Soc.* **50** (1967) 288.
7. K. ANDO, Y. OISHI and Y. HIDAKA, *J. Chem. Phys.* **65** (1976) 2751.
8. R. E. CARTER and W. L. ROTH, in "Electromotive Force Measurements in High-Temperature Systems", edited by C. B. Alcock (Elsevier, 1968) p. 125.
9. Y. SAKKA, Y. OISHI and K. ANDO, *Bull. Chem. Soc. Jpn.* **55** (1982) 420.
10. Y. OISHI, K. ANDO, H. KUROKAWA and Y. HIRO, *J. Amer. Ceram. Soc.* **66** (1983) C-60.
11. J. A. KILNER and R. J. BROOK, *Solid State Ionics* **6** (1982) 237.

Received 4 June  
and accepted 3 July 1984